ARTICLE

Optical and Mechanical Properties of Ramie Fiber/Epoxy Resin Transparent Composites

Chunhua Liu[1], Dongfang Zou[1], Qinqin Huang[1], Shang Li[2], Xia Zheng[1] and Xingong Li[1],*

[1]College of Materials Science and Engineering, Central South University of Forestry and Technology, Changsha, 410004, China

[2]College of Foreign Languages, Central South University of Forestry and Technology, Changsha, 410004, China

*Corresponding Author: Xingong Li. Email: lxgwood2021@163.com

ABSTRACT

The residual resources of ramie fiber-based textile products were used as raw materials. Ramie fiber felt (RF) was modified by $NaClO_2$ aqueous solution and then impregnated with water-based epoxy resin (WER). RF/WER transparent composite materials were prepared by lamination hot pressing process. The composite materials' color difference, transmittance, haze, density, water absorption, and mechanical properties were determined to assess the effects of $NaClO_2$ treatment and the number of ramie fiber layers on the properties of the prepared composites. The results showed significantly improved optical and mechanical properties of the RF/WER transparent composites after $NaClO_2$ treatment. With the increase of ramie fiber layers, the composites' whiteness, transmittance, and water absorption decreased while the haze increased. For material with three layers, the optical transmittance in the visible light region was 82%, and the haze was 96%, indicating the material has both high transmittance and high haze characteristics. The tensile strength increases with the increase of the number of layers, and the tensile strength of the composite with six layers is 243 MPa. This study broadens the scope of application of ramie fiber as a new option for home decoration materials.

KEYWORDS

Ramie fiber; water-based epoxy; transparent composites; transmittance; haze; tensile strength

1 Introduction

Driven by the concepts of environmental protection and sustainable development, there is growing interest in the development of natural fiber-reinforced polymer materials [1–3]. Compared with synthetic fibers, natural fibers are abundant, low-cost, and renewable resources [4]. Among the numerous hemp fibers, ramie fiber has outstanding performance. It has high cellulose content and is the only hemp fiber that can be spun in a single fiber state, so it is recognized as the king of natural fibers [5,6]. Ramie fiber is well suited for reinforced composites because of its fast heat dissipation, high mechanical strength, and antibacterial and corrosion resistance [7,8]. Chenniappan et al. [9] made composites of ramie fibers pretreated by hybridization and 2 wt% of aqueous NaOH solution and the materials exhibited a tensile strength of 120 MPa. Zulkifli et al. [10] found that the number of ramie woven layers and the weight of ramie fibers significantly affected the tensile and flexural strength of prepared composites, and the five-layer ramie woven composites had the highest tensile strength. Debeli et al. [11,12] found that alkali

treatment combined with $(NH_4)_2HPO_4$ effectively reduced the hydrophilicity of the ramie fiber surface and enhanced the tensile, fracture, and impact damage properties of ramie/PLA composites. Most studies on ramie fiber-reinforced polymer materials have focused on the optimization and enhancement of the fiber fabrication process, interfacial compatibility between fiber and matrix, and physical and mechanical properties of the material [13], with few studies of transparent ramie fiber composites, thus limiting application.

Transparent wood is one of the most widely researched bio-based transparent materials because of its high light transmittance and haze, low thermal conductivity, and excellent mechanical properties, suggesting a high potential for use as an optical material [14]. Functional modification can further enhance the application value of transparent wood. Wang et al. [15] studied a photochromic transparent wood for light switchable smart windows. Mi et al. [16] studied a transparent, strong, and insulating transparent wood for energy-efficient windows. Montanari et al. [17] studied an energy-storing, transparent wood based on PEG phase change material. However, the removal of lignin during the preparation of transparent wood can destroy the wood structure. In addition, impregnating resin into some solid wood will result in uneven resin impregnation due to poor permeability, which ultimately affects the performance of the product [18]. As a result, transparent wood can only be prepared at a small scale, using wood substrate with good permeability, making it difficult to achieve mass production and limiting the diversity of transparent wood applications.

Ramie fiber is a lignocellulosic fiber whose main components are cellulose (71%) and lignin (10%) [19]. The wood-like structure suggests that ramie fibers could be used to prepare transparent materials using the same methods developed to prepare transparent wood. Ramie fiber has a relatively large specific surface area and good dimensional stability, making the delignification treatment and the high polymer impregnation treatment relatively easy [20]. Unlike wood, ramie fiber should not be vulnerable to the process defects of wood, which can easily crack or exhibit difficulties with resin impregnation. The advantages of ramie fiber should allow mass manufacture of products of any required size to meet the needs of customers [21]. This study modified ramie fiber felt by $NaClO_2$ aqueous solution and then impregnated with water-based epoxy resin to prepare fiber-based transparent composites by hot press molding. To investigate the effects of $NaClO_2$ treatment and the number of pressed layers on the optical properties of the composites, the water absorption and mechanical properties was determined. The results of this work provide the basis for the preparation of fiber-based transparent composites.

2 Materials and Methods

2.1 Test Materials

Water-based epoxy resin (WER) was purchased from Yiwei Color World Coating Co. (Ningbo, China), with parameters of epoxy equivalent, 210–244 g/eq; viscosity of thermosetting resin, 84 Pa·s; and solid content, 64%. Ramie fiber felt (RF) was purchased from the Institute of Hemp, Chinese Academy of Agricultural Sciences (Changsha, China). The structure is non-woven fabric with surface density of 40 g/m^2 and thickness of 0.18 mm. Sodium chlorite ($NaClO_2$) analytically pure, was purchased from the Shanghai Maclean Biochemical Technology Co. (Shanghai, China). Glacial acetic acid (CH_3COOH), chemically pure, was purchased from Hunan Huihong Reagent Co. (Changsha, China). Distilled water was prepared in the laboratory.

2.2 Equipment

The following equipment was used in this work: QD86107 Hot Press, Suzhou Synergy Machine Manufacturing Co. (China); Sigma 300 scanning electron microscope, Carl Zeiss AG, Germany; DCS-R-100 universal mechanical testing machine, Shimadzu, Japan; NR-110 handheld color difference analyzer, Shenzhen Sanench Technology Co. (China); Density meter, Beijing Yitano Electronic Technology Co.

(China); Double-beam UV-Visible Spectrophotometer TU-1901, Shanghai Huyue Ming Scientific Instruments Co. (China); D8-discover X-ray diffractometer, Bruker, Germany; Nexus 670 FTIR-Raman spectrometer, Thermo Nicolet, USA.

2.3 Composite Material Preparation

Fig. 1 shows the process flow diagram for the preparation of RF/WER composite material. After the RF was dried, 5 wt% $NaClO_2$ aqueous solution was prepared at a ratio of RF to solution of 1:30. The pH value of $NaClO_2$ solution was adjusted to 4.6 with glacial acetic acid solution, the solution was put into a water bath, heated to 60°C, the weighed RF was added, and the solution was incubated in the water bath for 60 min. After the reaction, the RF was filtered after delignification, rinsed with distilled water three times, and then dried. Samples were prepared with three layers of untreated ramie fibers and three, four, five, six layers of delignified ramie fibers, and soaked in 580 g/m^2 water-based epoxy resin matrix solution for three minutes. The samples were then tiled and dried at room temperature for 12 h. Finally, the resin was hot pressed in a hot press to allow the resin to flow and densely polymerize with the ramie fiber to obtain RF/WER composite. The hot pressing process parameters were as follows: hot pressing pressure of 5 MPa, hot pressing temperature of 125°C, and hot pressing time of 20 min. The samples without $NaClO_2$ treatment were named RFWER-0, and the samples after $NaClO_2$ treatment were named RFWER-1, RFWER-2, RFWER-3, and RFWER-4, for the samples prepared with different numbers of layers.
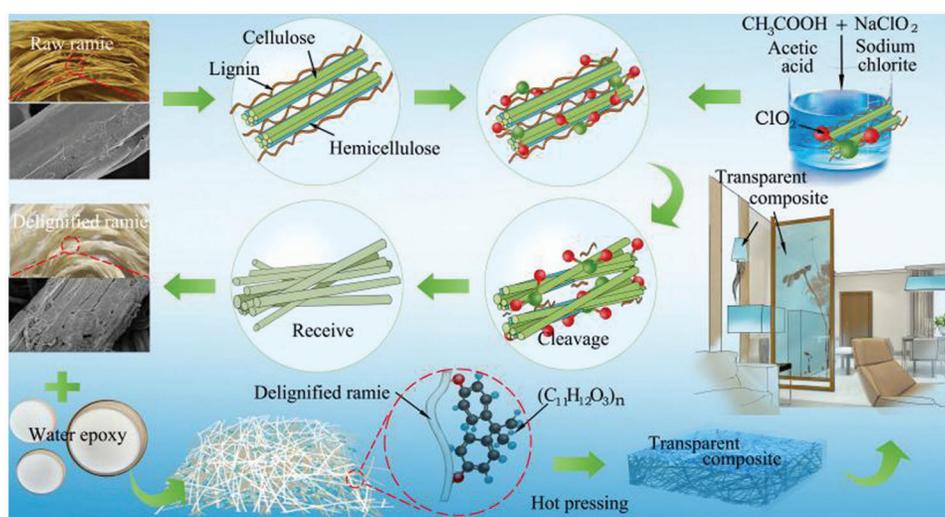

Figure 1: RF/WER composite preparation

2.4 Performance Testing and Characterization

Color difference was assessed using a NR-110 handheld color difference analyzer (Sanenchi) to analyze the effect of $NaClO_2$ treatment and the number of pressed layers on the color phase of the composites.

Samples were prepared according to GB/T 2410-2008 and tested with a double-beam UV-Vis spectrophotometer (TU-1901). The specimens were fixed on the UV spectrophotometer fixture, the integration sphere was selected as an accessory, barium sulfate powder was selected as the white plate, and the specimen side length was 20 mm.

The tensile properties of the materials were tested using a DCS-R-1000 mechanical testing machine according to GB/T 1040.3-2006. The load cell was a spoke type load cell and testing was performed with

a loading speed of 10 mm/min using a sample size of 150 mm × 20 mm. The test was performed on at least five parallel samples and the average value was taken.

The density of the material was determined according to Archimedes' method using an E-Terno density tester. The change in mass of the specimen was determined before and after water absorption according to GB/T 17657-2013.

The infrared spectrum was measured by Nexus670 Fourier infrared-Raman spectrometer. To do this, powder samples were prepared, KBr tablet was pressed, and the sample was measured at wavelength range of 4000–500 cm.

The crystalline structure of samples was analyzed using a German D8Discover X-ray diffractometer with a Cr target, Ni filter, a tube voltage of 25 kV, a tube current of 30 mA, and an integration time of 100 s.

The surface morphology of the original ramie fiber and the ramie fiber samples treated with $NaClO_2$ was analyzed by scanning electron microscopy (Sigma 300 scanning electron microscope). The test voltage was 20 kV, and the samples were sprayed with gold before analysis.

3 Results and Discussion

3.1 Color Difference Analysis of Composite Materials

The color of RF was measured before and after $NaClO_2$ treatment, as shown in Fig. 2. The results showed that after $NaClO_2$ treatment, the RF became significantly whiter. This was caused by the reaction between sodium chlorite and glacial acetic acid under heating conditions, which released chloric acid that decomposed into chlorine dioxide; the chlorine dioxide solution separated the chromogenic group lignin [22,23]. The color difference values of the prepared samples were measured and are shown in Table 1. The lightness value (L) of the RF/WER composite was significantly improved after $NaClO_2$ treatment, and the red-green value (a), yellow-blue value (b), and whiteness value (Wh) were significantly reduced. The surface color of RF/WER composites showed variability with increased number of pressed layers increased. As shown in Fig. 2d, analysis of the composites prepared with different number of layers showed gradually decreased transparency of the composites with increased number of layers of the substrate. The values of the color parameters (L, a, b, Wh) of the RFWER-1-RFWER-4 samples are listed in Table 1. As shown, with the increase in the number of pressed layers, the lignin residue gradually increased and the L value showed a decreasing trend, from 53.48 (RFWER-1) to 50.15 (RFWER-4). There was also a decrease in brightness. B values showed an upward trend, from 17.81 (RFWER-1) to 19.28 (RFWER-4), with yellow-blue deepening. The whiteness values decreased gradually from 46.37 (RFWER-1) to 33.08 (RFWER-4). The variation of color parameters showed that the surface color of RFW/ER transparent composites showed a systematic trend with increasing number of pressed layers, but the degree of variation was not significant.
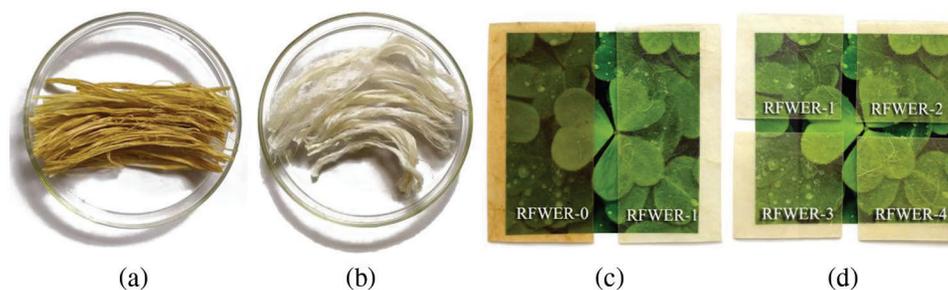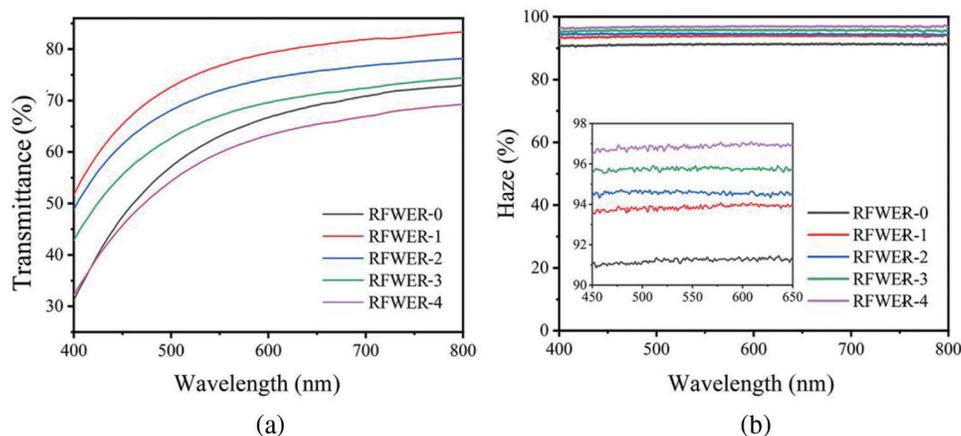

(a)   (b)   (c)   (d)

Figure 2: Untreated ER (a) and $NaClO_2$-treated ER (b). Untreated and $NaClO_2$-treated composites (c) and Composites with different number of pressed layers (d)

Table 1: RF/WER composite color data

Code	L	a	b	Wh
RFWER-0	51.81	1.72	18.79	41.21
RFWER-1	53.48	1.55	17.81	46.37
RFWER-2	52.76	1.61	18.30	45.38
RFWER-3	51.79	1.79	18.82	41.15
RFWER-4	50.15	2.32	19.28	33.08

3.2 Analysis of Optical Properties of Composite Materials

Fig. 3a shows the light transmittance curves of RF/WER transparent composites. At 555 nm, the optical transmittance of RFWER-0, RFWER-1, RFWER-2, RFWER-3 and RFWER-4 were 62%, 77%, 72%, 67%, and 60%, respectively. The optical transmittance of RF/WER composites treated with $NaClO_2$ increased by at least 15% compared to RF/WER composites without treatment. This change can be attributed to the removal of the light-absorbing chromophores of lignin in RF by $NaClO_2$ treatment [24]. However, the light transmission rate decreased as the number of layers increased. This is because when the number of pressed layers increases, the thickness of the material also gradually increases, so light propagates deeper inside the sample, scattered light increases, and transmitted light decreases. Thus, the light transmission rate of the composite shows a decreasing trend.

Figure 3: RF/WER composite transmittance (a) and haze (b)

At 555 nm wavelength, the haze values of RFWER-0, RFWER-1, RFWER-2, RFWER-3, and RFWER-4 were 90%, 93%, 94%, 95%, and 96%, respectively. The haze of RF/WER composites treated with $NaClO_2$ increased by at least 3% compared to RF/WER composites without any treatment. Additionally, the haze of the composites increased from 93% to 96% as the number of pressed layers increased. The observed haze increase corresponds to the number of layers (thickness) for the $NaClO_2$ treated and compacted samples, as additional layers increase the scattering light at the interface between RF and WER. RF/WER composites exhibit both high transmittance and high haze. Materials with these characteristics can be used to ensure privacy and a certain degree of light transmission [25]. For use as interior design materials, RF/WER transparent composites could be prepared with different light transmittance and haze values by adjusting the number of pressed layers to meet specific design needs.

3.3 Analysis of Mechanical Properties of Composite Materials

The tensile strength of fiber-reinforced composites depends on the degree to which the matrix transmits the load to the reinforcing fibers. The degree of load transmission is related to factors such as the dispersion of the fibers and the strength of interfacial bonding between the fibers and the matrix resin [26,27]. RF can enhance the mechanical properties of the resin matrix because the resin matrix transfers part of the load to the reinforcing fibers, and the interface mediates this transfer effect between the two phases. As shown in Fig. 4a, the tensile strength of RF/WER composites increased by about 19% after RF was treated with $NaClO_2$; this is obvious for RFWER-0 and RFWER-1. This result indicates that reduced hydrophilic groups of RF after delignification treatment with enhanced interfacial bonding strength to hydrophobic WER. Thus the composite has improved efficiency of dispersion of the damage load when damaged by external forces, for excellent robustness [28]. The tensile strength of the composites increased with the increase of the number of pressed layers. This is because RF reinforces fibers and the matrix shares the tensile external force, so the force acting on the matrix is uniformly dispersed, thus increasing the overall tensile strength of the composite.
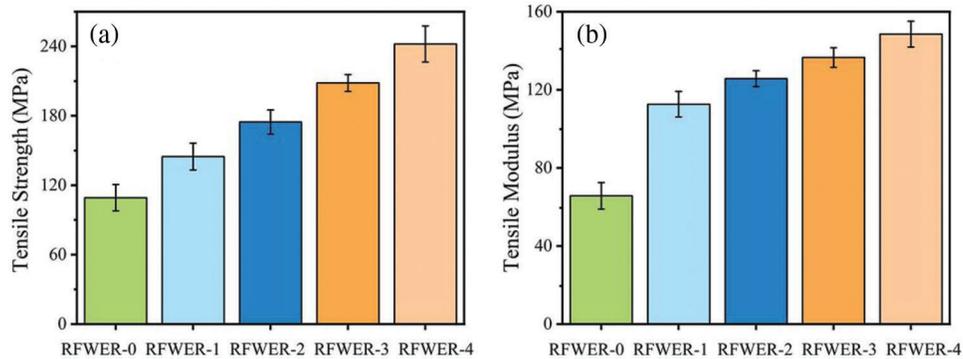
Figure 4: RF/WER composite tensile strength (a) and tensile modulus (b)

The RF in the composite will limit the tensile deformation of the epoxy resin, so smaller stresses cannot cause deformation in the composite. As shown in Fig. 4b, the tensile modulus values of the composites were also significantly improved after $NaClO_2$ treatment, indicating that $NaClO_2$ treatment allowed the composites to more effectively transfer the damage stress and protect the composites. At the same time, the elastic modulus values of the composite increased as the number of pressed layers increased. This reflects the increase in material strength caused by the increase in the amount of fiber, as increased fiber hinders the deformation of resin matrix composites. Given these mechanical properties, isotropic RF/WER transparent composites made of disordered fibers are more suitable for home decoration applications than anisotropic wood-based transparent composites.

3.4 Analysis of Density and Water Absorption of Composite Materials

The effects of $NaClO_2$ treatment and the number of pressed layers on the density and water absorption changes of RF/WER composites were determined and the results are shown in Figs. 5a and 5b. The density values of the composites increased after treatment of RF with $NaClO_2$. The density values decreased with the increase of the number of pressed layers, but the change in amplitude was between 1%–3%, indicating there were no significant changes.
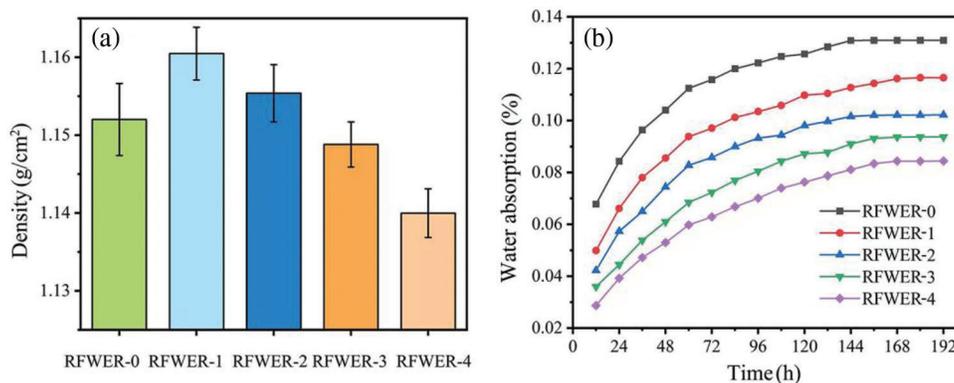
Figure 5: RF/WER composite density (a) and water absorption (b)

With the increased number of pressed layers, composite mass increased significantly. The magnitude of water absorption was positively correlated with the amount of exposed hydrophilic groups exposed. WER is a hydrophobic material with very low water absorption. When RF is compounded with WER, WER can penetrate into the RF cavity structure, increasing the hydrophobicity of the RF interface and thus effectively impeding the entry of water molecules into the composite interior. With $NaClO_2$ treatment and increased number of pressed layers, the barrier to water entry increases. As shown in Fig. 5b, when the composite material increased from three layers to four layers, the water absorption significantly decreased, from 13.09% to 10.21%. All three major components of RF (cellulose, hemicellulose, and lignin) contain a large number of hydroxyl groups that readily absorb water [29]. When the number of pressing layers continues to increase, the water resistance of the composite is not further improved. For example, when the number of RF/WER composite layers increases from five to six, its water absorption decreases from 9.36% to 8.12%, a change of only 1.24%. The mechanical properties, dimensional stability, and fungal corrosion resistance of RF/WER transparent composites will decrease after water absorption [30], so utilization of an appropriate number of RF pressed layers is required.

3.5 IR Analysis of RF before and after $NaClO_2$ Treatment

Fig. 6 shows the infrared spectral data for RF samples before and after $NaClO_2$ treatment. The results showed the absorption vibration peak of ramie fiber aromatic ring skeleton at 1549 cm^{-1}, the absorption peak of methyl and methylene bending vibration at 1435 cm^{-1}, and the peaks corresponding to C=O bond stretching vibration in lignin at 1624 and 1321 cm^{-1}; these four peaks are all characteristic peaks of lignin. Comparison of the IR spectra before and after treatment revealed that the characteristic peaks of lignin became weaker or disappeared after $NaClO_2$ treatment, indicating the effective removal of lignin from the RF. The characteristic peak of pectin at 1639 cm^{-1} corresponds to the stretching vibration peak of the carboxyl group of uronic acid in pectin. After $NaClO_2$ treatment, the characteristic peak of pectin decreased in intensity, indicating decreased content of pectin in RF. The absorption peak at about 1738 cm^{-1} corresponds to the stretching vibration of acetyl C=O, a characteristic peak of hemicellulose. This peak disappeared after $NaClO_2$ treatment, indicating the significant removal of hemicellulose. To summarize [31,32], the results indicate the removal of non-cellulose components such as lignin, hemicellulose, and pectin from RF after $NaClO_2$ treatment.
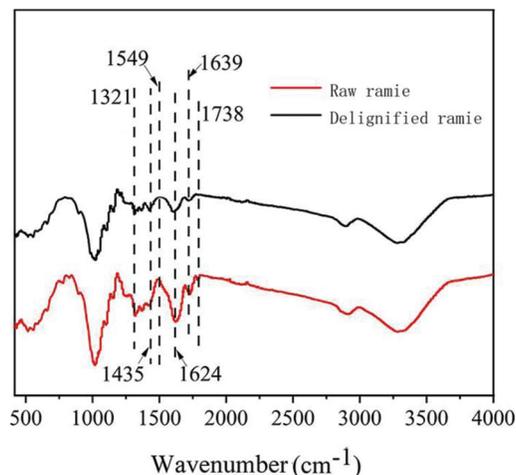
Figure 6: Infrared spectra of RF before and after NaClO$_2$ treatment

3.6 RF X-ray Diffraction Analysis before and after NaClO$_2$ Treatment

Fig. 7 shows the X-ray diffraction patterns of RF samples before and after NaClO$_2$ treatment. As seen in Fig. 7, the diffraction peaks in the amorphous region of cellulose near 18° and the diffraction peaks in the crystalline region of cellulose between 22 and 23° all showed a significant increase. This rise of diffraction peaks indicates that NaClO$_2$ treatment largely removes lignin and hemicellulose, pectin, and wax layers from RF, destroying the amorphous and crystalline regions of cellulose [33]. The peak splitting method was applied and revealed an increase in crystallinity of RF after NaClO$_2$ treatment from 69.77% to 94.83%. Together, these results indicate that treatment with NaClO$_2$ facilitates the removal of lignin, hemicellulose, and pectin from RF, thus changing cellulose polymerization chains and surface morphology [34]. This improves the compatibility of the fiber with the matrix resin, to greatly improve the material's overall optical and mechanical properties. Additionally, the NaClO$_2$ treatment disrupted the hydrogen bonds, enhanced the sliding ability between the microprotofibrils, and adjusted the tension between the microprotofibrils and macromolecules, for increased fiber strength [35]. Overall, the results show that NaClO$_2$ treatment can improve the optical and mechanical properties of RF/WER transparent composites. These conclusions are consistent with the results obtained by infrared spectroscopy.
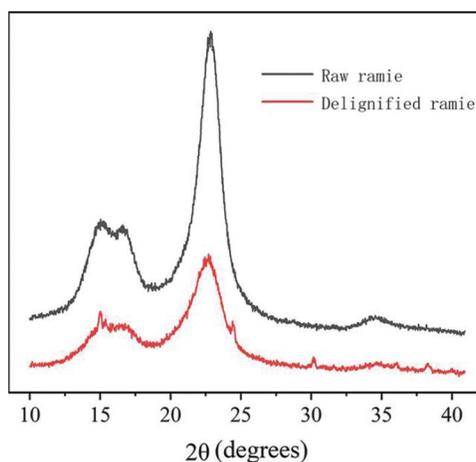

Figure 7: XRD patterns of RF before and after NaClO$_2$ treatment

3.7 Microscopic Morphology of RF and Composite Tensile Sections before and after NaClO$_2$ Treatment

Fig. 8 shows the scanning electron micrographs of RF and composites before and after NaClO$_2$ treatment. As shown in Figs. 8a and 8d, the RF surface appeared smooth, but NaClO$_2$ treatment resulted in a rough RF surface with many fine grooves on the surface. This is because NaClO$_2$ treatment removes lignin, hemicellulose, pectin, and other substances on the RF surface, and promotes RF fibrillation [34]. The rough and large specific surface area of RF after NaClO$_2$ treatment can facilitate the penetration of resin solution into the composite interior, allowing the formation of more mechanical "interlocking" structures between RF and WER. This results in stronger mechanical coupling, with an improved RF-WER bonding interface and composite mechanical properties. As shown in Figs. 8b and 8c, the RF surface on the tensile section of the composites prepared by RF without NaClO$_2$ treatment appeared smooth, with almost no WER adhesion. Obvious gaps were observed between RF and WER at the interface, indicating a weak bonding interface. When damaged by tensile external forces, RF can be easily "pulled off" from the WER and RF cannot transfer the damage stress well, so the composite material exhibits low tensile strength. As shown in Figs. 8e and 8f, there is obvious WER adhesion on the surface of RF fibers on the tensile section of the composites of NaClO$_2$-treated RF, with no obvious gap at the interface between RF and WER. This indicates an improved RF and WER bonding interface [36], so when the composites are damaged by tensile external force, RF fibers can help transmit the damage stress. This result is consistent with the observed improved mechanical properties of the composite.
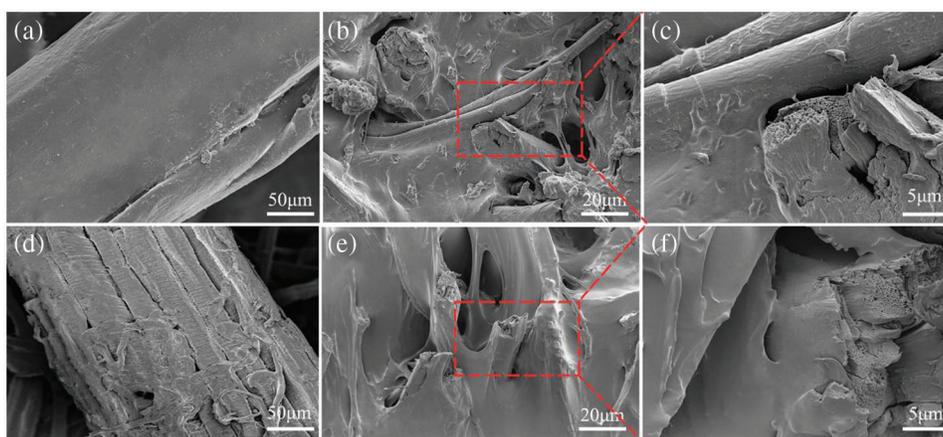

Figure 8: SEM images of untreated RF (a) and NaClO$_2$-treated RF (d). SEM images of untreated composites (b), (c) and NaClO$_2$-treated composites (e), (f)

4 Conclusions

In summary, compared with untreated RF/WER composites, the optical and mechanical properties of composites treated with NaClO$_2$ were significantly improved, with a 15% increase in transmittance, a 3% increase in haze, and a 19% increase in tensile strength. The number of layers significantly affected the properties of RF/WER composites. With an increase in the number of layers, the water absorption, whiteness value, and light transmission of the composites decreased and yellow-blue, red-green, haze values, and tensile properties increased. Composite materials can be applied as home decoration materials by tailoring the light transmission rate, haze value, and mechanical strength to meet different interior design needs by adjusting the number of pressed layers. This work provides the scientific basis for the preparation of fiber-based transparent composite materials.

Conflicts of Interest: The authors declare that they have no conflicts of interest to report regarding the present study.

References

1. Sun, Z. (2018). Progress in the research and applications of natural fiber-reinforced polymer matrix composites. *Science and Engineering of Composite Materials, 25(5),* 835–846. https://doi.org/10.1515/secm-2016-0072

2. Kabir, M., Wang, H., Lau, K., Cardona, F. (2012). Chemical treatments on plant-based natural fibre reinforced polymer composites: An overview. *Composites Part B: Engineering, 43(7),* 2883–2892. https://doi.org/10.1016/j.compositesb.2012.04.053

3. Gao, C., Wu, Y., Xie, H. (2023). Fully bio-based composites of poly (lactic acid) reinforced with cellulose-graft-poly-(ε-caprolactone) copolymers. *Journal of Renewable Materials, 11(3),* 1137–1152. https://doi.org/10.32604/jrm.2022.021473

4. Arpitha, G., Yogesha, B. (2017). An overview on mechanical property evaluation of natural fiber reinforced polymers. *Materials Today: Proceedings, 4,* 2755–2760. https://doi.org/10.1016/j.matpr.2017.02.153

5. Listyanda, R. F., Wildan, M. W., Ilman, M. N. (2020). Preparation and characterization of cellulose nanocrystal extracted from ramie fibers by sulfuric acid hydrolysis. *Heliyon, 6(11),* e05486. https://doi.org/10.1016/j.heliyon.2020.e05486

6. Young, C. H., Soon, L. J. (2012). Effects of surface treatment of ramie fibers in a ramie/poly(lactic acid) composite. *Fibers and Polymers, 13(2),* 217–223. https://doi.org/10.1007/s12221-012-0217-6

7. Ramesh, M., Rajeshkumar, L., Balaji, D. (2021). Mechanical and dynamic properties of ramie fiber-reinforced composites. *Mechanical and Dynamic Properties of Biocomposites,* 275–291. https://doi.org/10.1021/acsomega.0c00506

8. Hajime, K., Akira, F. (2008). Wood-based epoxy resins and the ramie fiber reinforced composites. *Environmental Engineering and Management Journal, 7(5),* 517–523. https://doi.org/10.30638/eemj.2008.074

9. Chenniappan, T., Uttamchand, N. (2022). Vibrational analysis of glass/ramie fiber reinforced hybrid polymer composite. *Polymer Composites, 43(3),* 1395–1406. https://doi.org/10.1002/pc.26460

10. Zulkifli, D., Ilyas, R., Miftahul, J. (2021). Tensile and bending strength analysis of ramie fiber and woven ramie reinforced epoxy composite. *Journal of Natural Fibers, 18(12),* 2315–2326. https://doi.org/10.1080/15440478.2020.1726242

11. Debeli, D. K., Guo, J., Li, Z., Zhu, J., Li, N. (2017). Treatment of ramie fiber with different techniques: The influence of diammonium phosphate on interfacial adhesion properties of ramie fiber-reinforced polylactic acid composite. *Iranian Polymer Journal, 26(5),* 341–354. https://doi.org/10.1007/s13726-017-0524-2

12. Debeli, D. K., Zhang, Z., Jiao, F., Guo, J. (2019). Diammonium phosphate-modified ramie fiber reinforced polylactic acid composite and its performances on interfacial, thermal, and mechanical properties. *Journal of Natural Fibers, 16(3),* 342–356. https://doi.org/10.1080/15440478.2017.1423255

13. Cheng, P., Peng, Y., Wang, K., Le Duigou, A., Yao, S. et al. (2023). Quasi-static penetration property of 3D printed woven-like ramie fiber reinforced biocomposites. *Composite Structures, 303,* 116313. https://doi.org/10.1016/j.compstruct.2022.116313

14. Tong, J., Wang, X., Kuai, B., Gao, J., Zhang, Y. et al. (2021). Development of transparent composites using wheat straw fibers for light-transmitting building applications. *Industrial Crops and Products, 170,* 113685. https://doi.org/10.1016/j.indcrop.2021.113685

15. Wang, L., Liu, Y., Zhan, X., Luo, D., Sun, X. (2019). Photochromic transparent wood for photo-switchable smart window applications. *Journal of Materials Chemistry C, 7(28),* 8649–8654. https://doi.org/10.1039/C9TC02076D

16. Mi, R., Li, T., Dalgo, D., Chen, C., Kuang, Y. et al. (2020). A clear, strong, and thermally insulated transparent wood for energy efficient windows. *Advanced Functional Materials, 30(1),* 1907511. https://doi.org/10.1002/adfm.201907511

17. Montanari, C., Li, Y., Chen, H., Yan, M., Berglund, L. A. (2019). Transparent wood for thermal energy storage and reversible optical transmittance. *ACS Applied Materials & Interfaces, 11(22),* 20465–20472. https://doi.org/10.1021/acsami.9b05525

18. Wu, Y., Zhou, J., Yang, F., Wang, Y., Wang, J. et al. (2021). A strong multilayered transparent wood with natural wood color and texture. *Journal of Materials Science, 56(13),* 8000–8013. https://doi.org/10.1007/s10853-021-05833-1

19. Handika, S. O., Lubis, M. A. R., Sari, R. K., Laksana, R. P. B., Antov, P. et al. (2021). Enhancing thermal and mechanical properties of ramie fiber via impregnation by lignin-based polyurethane resin. *Materials, 14(22),* 6850. https://doi.org/10.3390/ma14226850

20. Cheng, P., Wang, K., Le Duigou, A., Liu, J., Liu, Z. et al. (2022). A novel dual-nozzle 3D printing method for continuous fiber reinforced composite cellular structures. *Composites Communications, 101448.* https://doi.org/10.1016/j.coco.2022.101448

21. Miao, C., Hui, L. F., Liu, Z., Tang, X. (2014). Evaluation of hemp root bast as a new material for papermaking. *BioResources, 9(1),* 132–142. https://doi.org/10.15376/biores.9.1.132-142

22. Okahisa, Y., Abe, K., Nogi, M., Nakagaito, A. N., Nakatani, T. et al. (2011). Effects of delignification in the production of plant-based cellulose nanofibers for optically transparent nanocomposites. *Composites Science and Technology, 71(10),* 1342–1347. https://doi.org/10.1016/j.compscitech.2011.05.006

23. Chen, X., Ge-Zhang, S., Han, Y., Yang, H., Ou-Yang, W. et al. (2022). Ultraviolet-assisted modified delignified wood with high transparency. *Applied Sciences, 12(15),* 7406. https://doi.org/10.3390/app12157406

24. Li, T., Zhu, M., Yang, Z., Song, J., Dai, J. et al. (2016). Wood composite as an energy efficient building material: Guided sunlight transmittance and effective thermal insulation. *Advanced Energy Materials, 6(22),* 1601122. https://doi.org/10.1002/aenm.201601122

25. Valadez-Gonzalez, A., Cervantes-Uc, J., Olayo, R., Herrera-Franco, P. (1999). Effect of fiber surface treatment on the fiber-matrix bond strength of natural fiber reinforced composites. *Composites Part B: Engineering, 30(3),* 309–320. https://doi.org/10.1016/S1359-8368(98)00054-7

26. Jacob, M., Thomas, S., Varughese, K. (2004). Natural rubber composites reinforced with sisal/oil palm hybrid fibers: Tensile and cure characteristics. *Journal of Applied Polymer Science, 93(5),* 2305–2312. https://doi.org/10.1002/(ISSN)1097-4628

27. Nam, S., Netravali, A. N. (2006). Green composites. I. physical properties of ramie fibers for environment-friendly green composites. *Fibers and Polymers, 7(4),* 372–379. https://doi.org/10.1007/BF02875769

28. Jiang, Y., Yarin, A. L., Pan, Y. (2020). Printable highly transparent natural fiber composites. *Materials Letters, 277,* 128290. https://doi.org/10.1016/j.matlet.2020.128290

29. Wang, D., Ling, Q., Nie, Y., Zhang, Y., Zhang, W. et al. (2021). *In-situ* cross-linking of waterborne epoxy resin inside wood for enhancing its dimensional stability, thermal stability, and decay resistance. *ACS Applied Polymer Materials, 3(12),* 6265–6273. https://doi.org/10.1021/acsapm.1c01070

30. Praveenkumara, J., Madhu, P., Mavinkere, R. S., Suchart, S. (2021). A review on extraction, chemical treatment, characterization of natural fibers and its composites for potential applications. *Polymer Composites, 42(12),* 6239–6264. https://doi.org/10.1002/pc.26312

31. Kabir, M. M., Wang, H., Lau, K. T., Cardona, F. (2013). Effects of chemical treatments on hemp fibre structure. *Applied Surface Science, 276,* 13–23. https://doi.org/10.1016/j.apsusc.2013.02.086

32. Wang, H. M., Postle, R., Kessler, R. W., Kessler, W. (2003). Removing pectin and lignin during chemical processing of hemp for textile applications. *Textile Research Journal, 73(8),* 664–669. https://doi.org/10.1177/004051750307300802

33. Ahmed, B., Wu, Q., Lin, H., Gwon, J., Negulescu, I. (2022). Degumming of hemp fibers using combined microwave energy and deep eutectic solvent treatment. *Industrial Crops and Products, 184,* 115046. https://doi.org/10.1016/j.indcrop.2022.115046

34. Yu, W., Wang, C., Yi, Y., Wang, H., Zeng, L. et al. (2020). Comparison of deep eutectic solvents on pretreatment of raw ramie fibers for cellulose nanofibril production. *ACS Omega, 5(10),* 5580–5588. https://doi.org/10.1021/acsomega.0c00506

35. Abe, K., Morita, M., Yano, H. (2018). Fabrication of optically transparent cotton fiber composite. *Journal of Materials Science, 53.* https://doi.org/10.1007/s10853-018-2309-1

36. Feng, T., Qin, J., Shao, Y., Jia, L., Hu, Y. (2019). Size-controlled transparent jute fiber for replacing transparent wood in industry production area. *Coatings, 9(7),* 433. https://doi.org/10.3390/coatings9070433